RAIRO-Oper. Res. 50 (2016) 375–386
DOI: 10.1051/ro/2015041

RAIRO Operations Research
www.rairo-ro.org

STRUCTURAL AND ENERGETIC COMPARISON OF THE COMPLEXES OF AMINOGLYCOSIDES WITH THE MODEL OF THE RIBOSOMAL A-SITE *, **

Marta Kulik[1,2] and Joanna Trylska[1]

Abstract. Understanding the interactions which govern aminoglycoside antibiotic binding to ribosomal RNA is essential to propose modifications of these antibiotics. We have investigated the hydrogen bond patterns, solvent accessibility, and stacking energies of the nucleobases in twelve different aminoglycoside-RNA crystal complexes. These analyses pointed to some antibiotic-induced RNA structural differences that depend on the type of bound aminoglycoside. The largest differences were in the hydrogen bonding pattern in the vicinity of the U1406 and U1495 base pairs, especially in the complexes with geneticin and modified paromomycin. The complexes that stand out were the ones with neamine and kanamycin. We found that the solvent-accessible surface area buried upon aminoglycoside binding to RNA increases with the number of aminoglycoside rings but its correlation with the net charge of the antibiotic or experimental binding free energies was weak. We also investigated the dependence of other aminoglycoside characterizing descriptors, such as the number of rings and total charge, on the experimentally determined Gibbs energies. The correlation of ΔG with the total charge had the coefficient of determination R^2 over 0.8–0.9, depending on experimental data set, and was the highest of all descriptors.

Mathematics Subject Classification. 92C05, 92C40.

Received September 8, 2015. Accepted September 21, 2015.

1. Introduction

Naturally obtained aminoglycosides have been used as antibiotics for more than 60 years. Their ability to eradicate bacteria encompasses not only the Gram-negative but also certain Gram-positive bacteria [20]. However, due to multiple resistance mechanisms developed by bacteria, the clinical efficacy of aminoglycosides has significantly decreased. To overpass this problem, it is essential to understand in detail the interactions between aminoglycosides and their binding site which govern the formation of the complexes. In this study, we focus on a class of aminoglycosides containing the 2-deoxystreptamine (2-DOS) moiety.

Keywords. Aminoglycosides, ribosomal RNA, A-site, solvent accessible surface area, hydrogen bonds, nucleobase stacking.

* *Authors acknowledge support from the National Science Centre (DEC-2012/05/B/NZ1/00035).*

** *Computational resources were provided by the University of Warsaw (ICM/KDM/G31-4).*

[1] Centre of New Technologies, University of Warsaw, Banacha 2c, 02-097 Warsaw, Poland. joanna@cent.uw.edu.pl

[2] Department of Chemistry, University of Warsaw, Pasteura 1, 02-093 Warsaw, Poland. m.kulik@cent.uw.edu.pl

Article published by EDP Sciences

Due to their polycationic nature, aminoglycosides have high affinity to the negatively charged phosphates in the nucleic acid backbone [20]. Therefore, electrostatic forces play the leading role in aminoglycoside binding [41]. The net positive charge of the antibiotic was found more important for its complexation than conformational matching with the target [4]. The mode of action of these antibiotics is based on the interference with bacterial protein synthesis. 2-DOS aminoglycosides noncovalently attach to the major groove of helix 44 of 16S ribosomal RNA in the bacterial 30S ribosomal subunit, the so-called A-site. These interactions induce flipping out of two adenines in the A-site (A1492 and A1493 using standard *E. coli* numbering). A1492 and A1493 are responsible for the incorporation of cognate aminoacylated-tRNA in the A-site. Consequently, the incorporation of the near-cognate and non-cognate tRNA becomes possible, and the accuracy of translation decreases [17]. This is the primary mode of translation inhibition by 2-DOS aminoglycosides even though they can also interfere, for example, with the self-assembly of the 30S ribosomal subunit.

Many crystal structures of aminoglycosides in the complexes with the *E. coli* and *T. thermophilus* ribosomes were obtained [8]. The 2-DOS aminoglycosides have been also crystalized with relatively short RNA oligonucleotides sequentially mimicking the ribosomal A-site. Such isolated A-site constructs, for example the Westhof's model [40], structurally resemble the A-site and bind 2-DOS aminoglycosides in the same manner as ribosomes. They have been exploited in both solution experiments to determine the thermodynamics of binding and computational studies to investigate the dynamics and energetics of aminoglycoside–A-site complexes. For example, molecular dynamics simulations with paromomycin [33] and amikacin [11] confirmed that the neamine core plays a role of an anchor in the A-site binding cleft. Several simulations of the A-site have been conducted with an emphasis on the movements of A1492 and A1493 bases [24,29,30,33,36]. Simulations also revealed that the presence of certain hydration sites correlates with aminoglycoside binding affinity [6,11,35]. The electrostatic component of the binding free energy of several aminoglycosides bound to the static A-site [44] or 30S subunit [28,44] was calculated using the implicit solvent Poisson–Boltzmann model of electrostatic interactions [16]. These computations have taken into account also the contributions from nonpolar interactions by correlating them with the solvent-accessible surface area that gets buried upon forming a complex. The Poisson–Boltzmann model was also combined with Brownian dynamics approach to study the association of aminoglycosides with RNA [9,10]. Electrostatics was also studied with the Exact Potential Multipole Moment method [27].

These computational studies complemented experimental assays on similar RNA constructs containing the A-site. Thermal denaturation and fluorescence studies [23,34,44], isothermal titration calorimetry [2,11,21,22,32], UV spectrometry [21,22], differential scanning calorimetry [21] and surface plasmon resonance experiments [1,43] predicted the free enthalpy of binding and dissociation constants of aminoglycoside complexes. Bacterial growth inhibition checks giving the minimum inhibitory concentration data against *E. coli* species are also available [1,15,31].

The purpose of this study was to compare the mode of aminoglycoside binding in twelve different aminoglycoside-RNA crystallographically resolved complexes. We investigated the conformational differences in RNA upon complexation with various 2-DOS aminoglycosides. The Westhof's construct, composed of about 45 nucleotides, reflects the A-site properties in the ribosome [40] and has been crystallized with each of the studied aminoglycosides. Thus, it provides a perfect tool to observe the structural changes in the A-site upon antibiotic binding. The structural changes were also compared with experimental free energies of binding and previous computational studies of such complexes.

2. Methods

According to the position of glycosidic linkages and the molecular backbone (2-deoxystreptamine or streptidine) aminoglycosides are frequently divided into three structural families [20] of which 4,5- and 4,6-disubstituted 2-deoxystreptamines were taken into account in this study. The representatives of those two families are shown in Figures 1 and 2.

The aminoglycoside complexes with Westhof's construct [37] were taken from X-ray structures, deposited in the RCSB database [3]: 2ET8 [13], 1MWL [39], 2G5Q [25], 2ESI [13], 4F8V [26], 1LC4 [38], 2ET3 [13], 2ET5 [13],

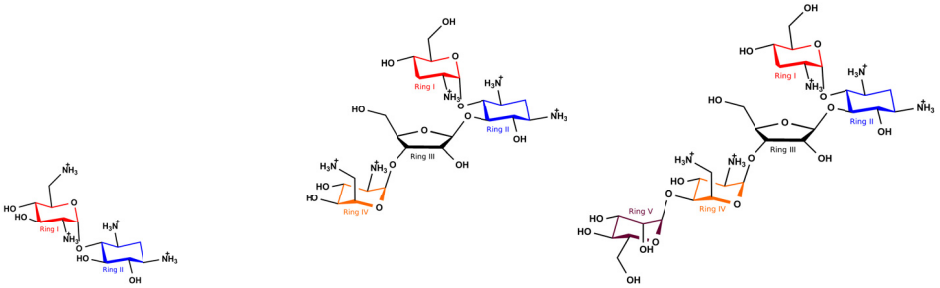

(A) Neamine (B) Paromomycin (C) Lividomycin A

FIGURE 1. 4,5-disubstituted 2-deoxystreptamines.

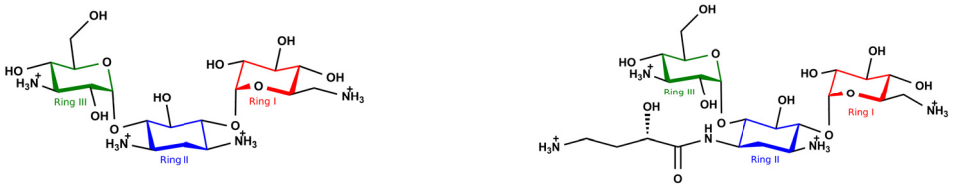

(A) Kanamycin A (B) Amikacin

FIGURE 2. 4,6-disubstituted 2-deoxystreptamines.

1J7T [37], 2BEE [12], 2ET4 [13], 2ESJ [13]. Each structure contains two mirrored A-sites. The RNA sequence is depicted in Figure 3b. All RNA constructs are identical except the 2ESI complex, in which additional uridines were removed to match all the other structures.

The preparation of structures was performed with the Amber11 package [5]. For all crystal structures, the hydrogen positions and ff99 Amber force field [42] parameters were assigned. The aminoglycosides were protonated according to their charge in neutral pH. The partial charges of aminoglycosides were determined with the AM1-BCC method [19]. The energy minimization of the complexes with restraints of 50 kcal/mol on non-hydrogen atoms of RNA and aminoglycosides was performed in explicit solvent. Sodium ions were used to neutralize the system. No additional ionic strength was applied.

The number of Watson–Crick (WC) and non-Watson–Crick (non-WC) hydrogen bonds, Coulomb energies, van der Waals (VDW) and stacking energies were determined with the MINT web server (Motif Identifier for Nucleic acids Trajectory) [14]. The resulting numbers of hydrogen bonds and energies have taken into account the interactions between RNA nucleobases only. Stacking per nucleotide was calculated within 10 Å distance cutoff from each nucleobase. The nucleobases contributing to stacking had the VDW energy below −0.5 kcal/mol. For these selected nucleobases, the Coulombic contribution was added to the stacking sum.

The solvent-accessible surface area (SASA) was calculated with VMD [18]. ΔSASA for each aminoglycoside was obtained by subtracting the SASA of the unbound aminoglycoside and RNA from the SASA of the complex, $\Delta\text{SASA} = \text{SASA}_{complex} - (\text{SASA}_{RNA} + \text{SASA}_{aminoglycoside})$.

3. Results and discussion

3.1. Hydrogen bond network between RNA base pairs

First, we compared the hydrogen bond patterns in twelve aminoglycoside-RNA complexes, each containing two aminoglycoside binding sites. According to our definition, the WC type hydrogen bonds are the bonds

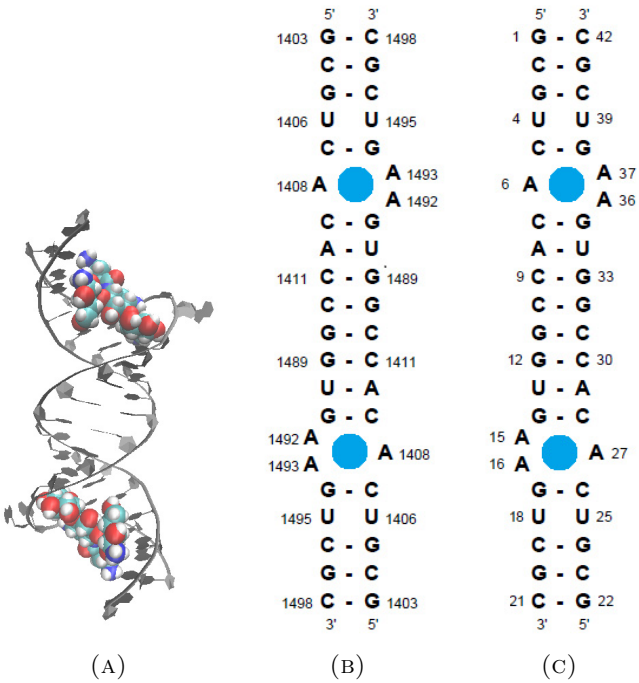

FIGURE 3. The structure of the Westhof's construct, present in all complexes used in the study. (A) Visualization of the complex with amikacin. RNA is in grey and amikacin as van der Waals spheres colored by atom type. The picture was generated with VMD [18]. (B) The RNA sequence and secondary structure with *E. coli* numbering. The dashed lines mark the Watson–Crick canonical hydrogen bonds. The aminoglycoside-binding pocket is schematically marked with a blue circle. (C) as (B) but with sequential numbering of nucleotides used further in this study.

fulfilling the hydrogen bond criteria and interacting *via* the WC edge of the nucleobase. This includes both canonical, as well as non-canonical (*e.g.* UU) hydrogen bonds if they interact via the WC edge.

In the dot-bracket notation shown in Table 1, in all the complexes, the WC base pairing is missing between A1492, A1493, and A1408. This is expected because these nucleotides form a bulge in order to accommodate aminoglycosides. In most of the complexes, the WC-edge non-canonical base pairs do not occur between U1406 and U1495. According to the dot-bracket image of base pairs (Tab. 1), formed between nucleotides from the opposite RNA strands, the complexes can be divided into three groups. In the first group, containing geneticin and modified paromomycin, all WC-edge hydrogen bonds are preserved, except these between adenines in the A-site bulge. The second group with kanamycin, tobramycin and neamine, does not show hydrogen bonds between U1406 and U1495 in one site of the complex. In the third group, containing the majority of complexes, the WC-edge hydrogen bonds between U1406 and U1495 in both sites are not present.

A more accurate analysis of hydrogen bonds classified as WC or non-WC is presented in Figures 4 and 5. In each figure, only one RNA strand is presented. In the non-WC variant, also the sugar and Hoogsteen edges can take part in forming hydrogen bonds. For the exact definition of the hydrogen bond types used in this study, see the MINT manual [14] at `http://mint.cent.uw.edu.pl`.

In Figure 4, the number of hydrogen bonds between bases ranged from 0 to 4. In most cases, three hydrogen bonds were present in the G-C pairing and two in the A-U pairing schemes. Four hydrogen bonds were observed in the complexes with neamine, kanamycin, neomycin, paromomycin and modified paromomycin. Deviations

TABLE 1. Dot-bracket representation of base pairs formed via WC edges in the complexes. The nucleotides A1492, A1493 and A1408 are marked red.

	Nucleotides 1–21 GCGUCACACCGGUGAAGUCGC	Nucleotides 22–42 GCGUCACACCGGUGAAGUCGC
get	(((((. (((((((. . (((((	))))) .)))))))) . .)))))
js4	(((((. (((((((. . (((((	))))) .)))))))) . .)))))
kan	(((. (. (((((((. . (((((	))))) .)))))))) . .) .)))
toy	(((. (. (((((((. . (((((	))))) .)))))))) . .) .)))
xxx	(((. (. (((((((. . (((((	))))) .)))))))) . .) .)))
akn	(((. (. (((((((. . (. (((	))) .) .)))))))) . .) .)))
liv	(((. (. (((((((. . (. (((	))) .) .)))))))) . .) .)))
lll	(((. (. (((((((. . (. (((	))) .) .)))))))) . .) .)))
nmy	(((. (. (((((((. . (. (((	))) .) .)))))))) . .) .)))
par	(((. (. (((((((. . (. (((	))) .) .)))))))) . .) .)))
rio	(((. (. (((((((. . (. (((	))) .) .)))))))) . .) .)))
sis	(((. (. (((((((. . (. (((	))) .) .)))))))) . .) .)))

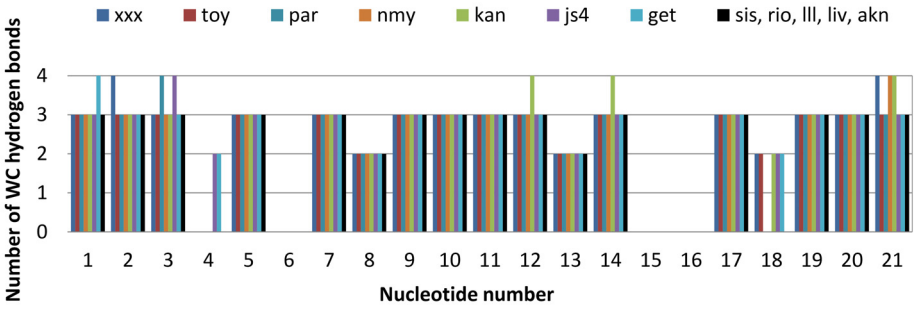

FIGURE 4. The number of WC hydrogen bonds created between base pairs of opposite RNA strands via the WC edge. For abbreviations of aminoglycoside names (see Tab. 2), and for nucleotide numbering (see Fig. 3c).

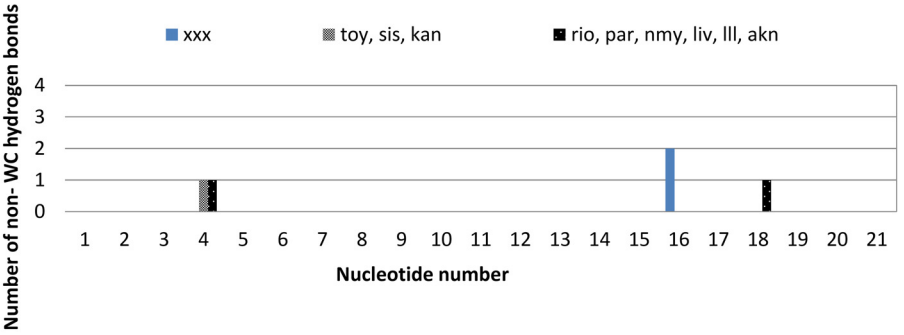

FIGURE 5. The number of non-WC hydrogen bonds created between opposite base pairs. For abbreviations of aminoglycoside names (see Tab. 2), and for nucleotide numbering (see Fig. 3c).

in the number of WC hydrogen bonds from the main pattern are present in the complex with kanamycin in the vicinity of the A-site and at the 3'-end of the construct. This effect is evoked by the presence of additional unspecifically bound antibiotic in one of the binding sites. More than three hydrogen bonds formed via WC edges are also visible in neamine, geneticin and neomycin complexes in the terminal regions of the construct, where nucleotide triples were detected. The above mentioned complexes can form hydrogen bonds between U1406 and U1495 in one or both A-sites of the RNA duplex.

There is a small number of non-WC hydrogen bonds in the structures. Almost all of them are found in the U1406 and U1495 base pair and contain interactions via the Hoogsteen edge. However, in the complex of neamine, two additional hydrogen bonds with A1493 are found. This is comprehensible, as one of the binding sites of this construct is not occupied by any aminoglycoside, which causes this A-site adenine to flip out and precludes its hydrogen bonding.

3.2. Stacking interactions

According to the procedure in MINT, the stacking interactions are calculated as the sum of Coulomb interaction energy and VDW energy between the nucleobases. The VDW energies represent the surface overlap of nucleobases. It is a better measure of stacking than a simple criterion based on the distances of the centers of mass of the nucleobases.

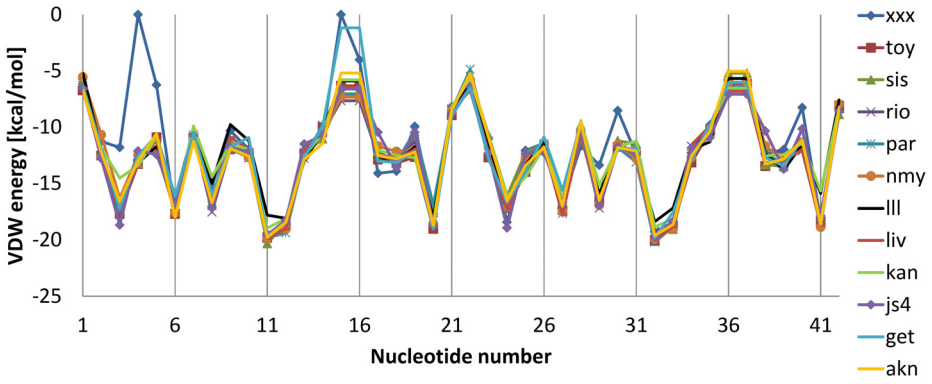

FIGURE 6. The VDW energies of each nucleotide in the RNA model of the A-site complexed with different aminoglycosides. For aminoglycoside names (see Tab. 2), and for nucleotide numbering (see Fig. 3c).

The VDW energies per nucleobase, presented in Figure 6, show that each nucleobase has favorable VDW interactions with the others in the A-site. Not surprisingly, the most visible changes in the energetics between two RNA strands are for the neamine complex. This is because neamine crystallized in only one of the two A-sites in the construct, so one of the sites is a free RNA. Among all structures, significantly less favorable VDW energies of nucleobases are found in the complex with geneticin in the second A-site region. This might be caused by high B-factor values of this site in the crystal structure [39].

Figure 7 presents the stacking energy, which is calculated as a sum of the Coulomb and VDW energies. For most nucleobases, more distant from the A-site bulge, the contributions from the Coulomb and VDW energies compensate and the resulting stacking energies are close to -5 kcal/mol or at least below zero. In some cases there is no stacking, which is in accord with what is observed by looking at the structure. For example, high energies are observed for the A1492 and A1493 region, in which the nucleobases do not stack. Figure 8 shows examples of the representative and atypical (for neamine) stacking energy pattern.

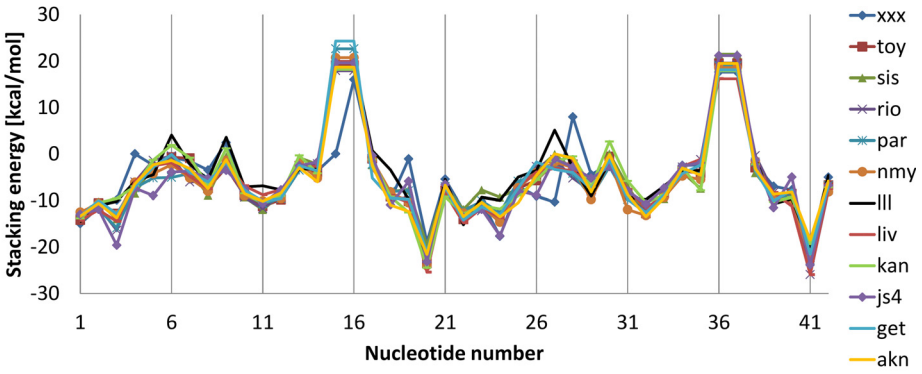

FIGURE 7. The stacking energy of each nucleotide in the RNA model of the A-site complexed with different aminoglycosides. For aminoglycoside names (see Tab. 2) and for nucleotide numbering (see Fig. 3c).

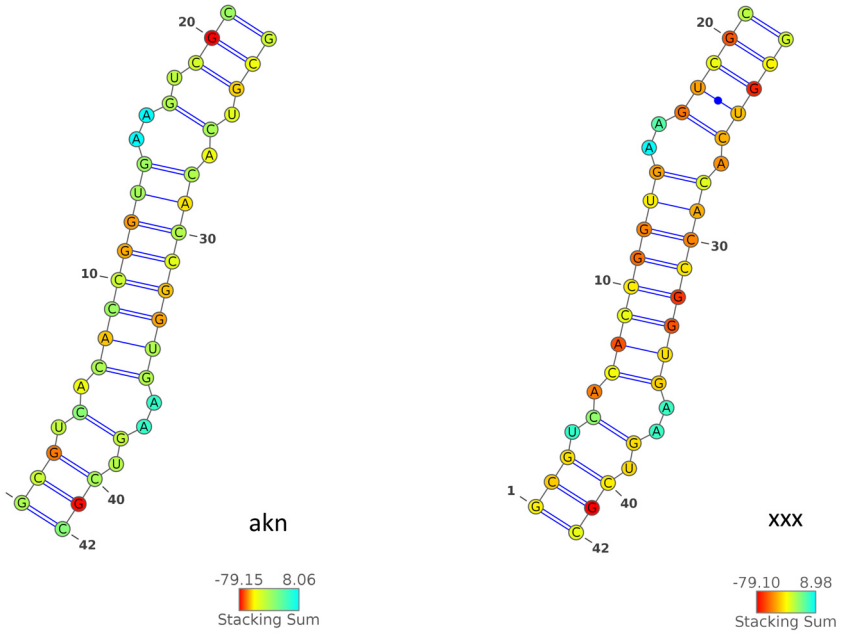

FIGURE 8. Visualization of the stacking energy for each nucleotide base in the amikacin (akn) and neamine (xxx) complexes. The picture was generated with VARNA [7].

3.3. Solvent-accessible surface area

The changes in solvent accessibility upon aminoglycoside binding, ΔSASA, for twelve aminoglycoside complexes are gathered in Table 2. The negative values of this parameter denote that during the formation of a complex a part of the solvent accessible surface area of the antibiotic and RNA get buried. The amount of ΔSASA depends on the size of the aminoglycoside; it increases with the number of rings which is presented in Figure 9. As expected, the most negative ΔSASA was determined for the lividomycin complex because this is

TABLE 2. The solvent-accessible surface area buried upon binding of an antibiotic (ΔSASA) and the experimentally determined Gibbs energies (ΔG). (a) Yang *et al.* [44]; (b) Alper *et al.* [1], Wong *et al.* [43] and (c) Pilch *et al.* [32]. The aminoglycosides are ordered according to their number of rings.

Aminoglycoside	No. of rings	Total charge [e]	ΔSASA [Å^2]	ΔG [kcal/mol]
Neamine (xxx)	2	4	−791	-7.03_a -6.96_b
Geneticin (get)	3	4	−832 −839	-6.71_a
Amikacin (akn)	3	4	−969 −982	
Kanamycin A (kan)	3	4	−823 −789	-6.64_a -6.47_b
Sisomicin (sis)	3	5	−768 −792	
Tobramycin (toy)	3	5	−805 −791	-7.54_a -7.94_b
Gentamicin C1A (lll)	3	5	−827 −801	-7.22_a -7.86_b
Ribostamycin (rio)	3	4	−719 −696	-6.64_a; -6.27_b -7.7_c
Paromomycin (par)	4	5	−928 −941	-8.77_a; -9.13_b -10.3_c
Neomycin B (nmy)	4	6	−925 −924	-10.56_a; -10.52_b -11.5_c
Paromomycin deriv. (js4)	4	7	−1041 −1079	
Lividomycin A (liv)	5	5	−1062 −1006	-10.5_c

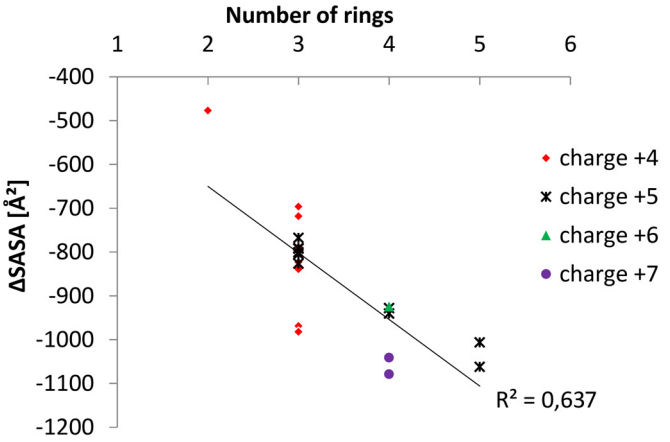

FIGURE 9. The relationship between ΔSASA and the number of aminoglycoside rings. The complexes are divided into groups of aminoglycosides with different net charges.

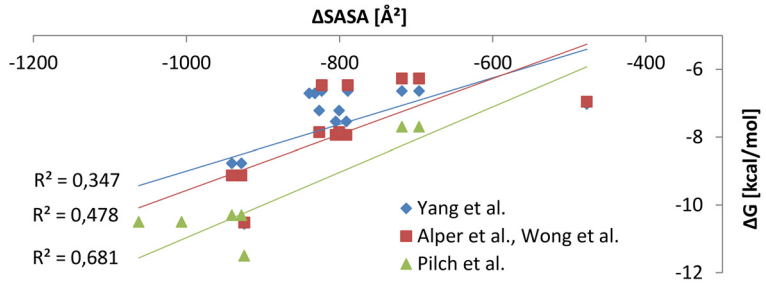

FIGURE 10. The correlation between ΔSASA and experimentally obtained Gibbs energies (ΔG) taken from the studies of Yang *et al.* [44]; Alper *et al.* [1], Wong *et al.* [43] and Pilch *et al.* [32].

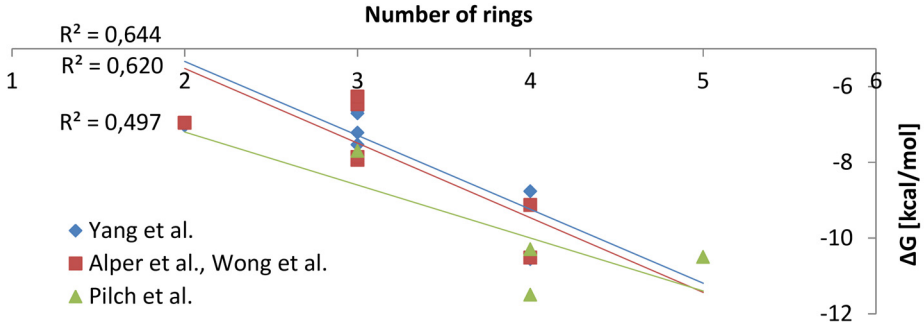

FIGURE 11. The correlation between the number aminoglycoside rings and experimentally obtained Gibbs energies (ΔG) taken from the studies of Yang *et al.* [44]; Alper *et al.* [1], Wong *et al.* [43] and Pilch *et al.* [32].

the largest of the studied antibiotics. However, the correlation of ΔSASA with the total aminoglycoside charge is weak and the R^2 is close to 0.3. This suggests that the electrostatic and non-polar contributions to binding free energies are not coupled.

The aminoglycoside binding to the RNA oligonucleotide construct of the A-site of *E. coli* was previously studied experimentally with fluorescence [44], surface plasmon resonance [1,43], isothermal titration calorimetry and UV melting assays [32]. The results of these experiments depend on many factors of the solution, such as the temperature, buffer composition, and pH. We are not able to reproduce these effects in our study. Nevertheless, the free energies of binding (ΔG) of aminoglycosides determined in these experiments should relate to the order of aminoglycoside binding, obtained in our computational analysis. The amount of ΔSASA relates relatively well to the experimental Gibbs energies obtained in one of the experimental studies, which is shown in Figure 10. However, the correlation of ΔG with the number of aminoglycoside rings is higher as shown in Figure 11.

3.4. Electrostatic interactions

At the same time, we compared the dependence of Gibbs energy derived from experimental data on the antibiotic net charge because the electrostatic interactions are known to be the main driving force in aminoglycoside association and formation of a stable complex. The correlation between the total aminoglycoside charges and their free energies of binding is shown in Figure 12. The net charge of an aminoglycoside correlates best with ΔG in comparison to other measures, namely ΔSASA and the number of rings.

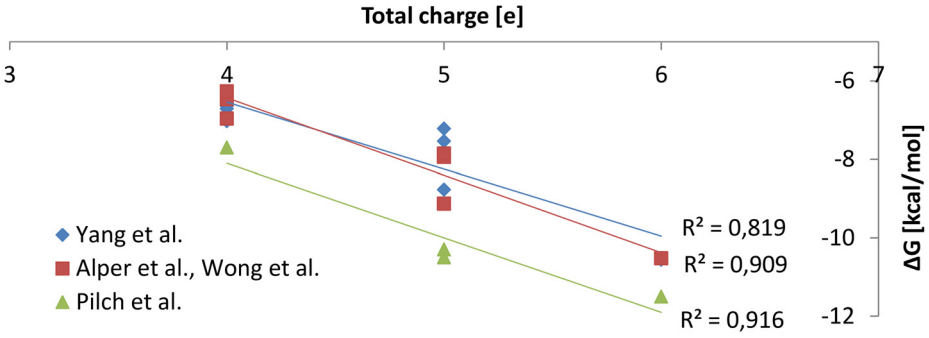

FIGURE 12. The correlation between the net charge of aminoglycosides and experimentally obtained Gibbs energies (ΔG) taken from the studies of Yang *et al.* [44]; Alper *et al.* [1], Wong *et al.* [43] and Pilch *et al.* [32].

4. Conclusions

We compared the hydrogen bonding pattern, solvent accessibility, and energetics in twelve aminoglycoside-RNA crystal complexes. The computations revealed differences in the RNA conformations in the complexes with different antibiotics. The most noticeable difference was observed in the number of hydrogen bonds, especially those located in the vicinity of the U1406 and U1495 base pair. In some complexes we also observed differences in hydrogen bonding pattern between the two symmetric A-sites. These changes are caused by the presence of an additional unspecifically bound kanamycin or lack of any bound aminoglycoside in one site, as in the case of neamine.

The Coulomb, VDW, and stacking energy calculations revealed structural differences of the nucleobases between sites and opposite strands of the construct. The complex containing neamine, the smallest aminoglycoside, was found to have the largest deviations in these energetic contributions.

For all the complexes we also compared SASA buried upon aminoglycoside binding. The solvent accessibility change, ΔSASA, correlates weakly with the experimental free energies of binding. SASA multiplied by the surface tension coefficient is often related to the change in non-polar contribution to binding. This suggests that indeed the electrostatic and not the non-polar component of aminoglycoside binding is the most dominant one in the crystal complexes. Indeed, in our previous study on the electrostatics of these complexes we observed correlations between the experimentally determined binding free energies and electrostatic contribution to binding, determined with the Exact Potential Multipole Moment method [27].

References

[1] P.B Alper, M. Hendrix, P. Sears and C.-H. Wong, Probing the Specificity of Aminoglycoside-Ribosomal RNA Interactions with Designed Synthetic Analogs. *J. Am. Chem. Soc.* **120** (1998) 1965–1978.

[2] C.M. Barbieri, A.R. Srinivasan and D.S. Pilch, Deciphering the origins of observed heat capacity changes for aminoglycoside binding to prokaryotic and eukaryotic ribosomal RNA a-sites: a calorimetric, computational, and osmotic stress study. *J. Am. Chem. Soc.* **126** (2004) 14380–14388.

[3] H.M. Berman, J. Westbrook, Z. Feng, G. Gilliland, T.N. Bhat, H. Weissig, I.N. Shindyalov and P.E. Bourne, The protein data bank. *Nucleic Acids Res.* **28** (2000) 235–242.

[4] K.F. Blount and Y. Tor, Using pyrene-labeled HIV-1 TAR to measure RNA-small molecule binding. *Nucleic Acids Res.* **31** (2003) 5490–5500.

[5] D.A. Case, T.A. Darden, T.E. Cheatham, C.L. Simmerling, J. Wang, R.E. Duke, R. Luo, M. Crowley, R.C. Walker, W. Zhang, K.M. Merz, B. Wang, S. Hayik, A. Roitberg, G. Seabra, I. Kolossváry, K.F. Wong, F. Paesani, J. Vanicek, X. Wu, S.R. Brozell, T. Steinbrecher, H. Gohlke, L. Yang, C. Tan, J. Mongan, V. Hornak, G. Cui, D.H. Mathews, M.G. Seetin, C. Sagui, V. Babin and P.A. Kollman, *Amber 11*. University of California, San Francisco.

[6] S.-Y. Chen and T.-H. Lin, A molecular dynamics study on binding recognition between several 4,5 and 4,6-linked aminoglycosides with A-site RNA. *J. Mol. Recognit.* **23** (2010) 423–434.

[7] K. Darty, A. Denise and Y. Ponty, VARNA: Interactive drawing and editing of the RNA secondary structure. *Bioinform.* **25** (2009) 1974–1975.

[8] N. Demeshkina, L. Jenner, E. Westhof, M. Yusupov and G. Yusupova, A new understanding of the decoding principle on the ribosome. *Nature* **484** (2012) 256–259.

[9] M. Długosz and J. Trylska, Aminoglycoside Association Pathways with the 30S Ribosomal Subunit. *J. Phys. Chem. B* **113** (2009) 7322–7330.

[10] M. Długosz, J.M. Antosiewicz and J. Trylska, Association of Aminoglycosidic Antibiotics with the Ribosomal A-Site Studied with Brownian Dynamics. *J. Chem. Theory Comput.* **4** (2008) 549–559.

[11] M. Dudek, J. Romanowska, T. Wituła and J. Trylska, Interactions of amikacin with the RNA model of the ribosomal A-site: computational, spectroscopic and calorimetric studies. *Biochimie* **102** (2014) 188–202.

[12] B. François, J. Szychowski, S.S. Adhikari, K. Pachamuthu, E.E. Swayze, R.H. Griffey, M.T. Migawa, E. Westhof and S. Hanessian, Antibacterial Aminoglycosides with a Modified Mode of Binding to the Ribosomal-RNA Decoding Site. *Angew. Chem., Int. Ed.* **43** (2004) 6735–6738.

[13] B. François, R.J. Russell, J.B. Murray, F. Aboul-ela, B. Masquida, Q. Vicens and E. Westhof, Crystal structures of complexes between aminoglycosides and decoding a site oligonucleotides: role of the number of rings and positive charges in the specific binding leading to miscoding. *Nucleic Acids Res.* **33** (2005) 5677–5690.

[14] A. Górska, M. Jasiński and J. Trylska, MINT: software to identify motifs and short-range interactions in trajectories of nucleic acids. *Nucl. Acids Res.* **43** (2015) e114.

[15] S. Hobbie, P. Pfister, C. Bruell, E. Westhof and E. Boettger, Analysis of the contribution of individual substituents in 4,6-aminoglycoside-ribosome interaction. *Antimicrob. Agents Chemother.* **49** (2005) 5112–5118.

[16] B. Honig and A. Nicholls, Classical electrostatics in biology and chemistry. *Science* **268** (1995) 1144–1149.

[17] J.L. Houghton, K.D. Green, W. Chen and S. Garneau-Tsodikova, The future of aminoglycosides: the end or renaissance? *Chem. Bio. Chem.* **11** (2010) 880–902.

[18] W. Humphrey, A. Dalke and K. Schulten, VMD – Visual Molecular Dynamics. *J. Mol. Graph.* **14** (1996) 33–38.

[19] A. Jakalian, B.L. Bush, D.B. Jack and C.I. Bayly, Fast, efficient generation of high-quality atomic charges. AM1-BCC model: I. Method. *J. Comput. Chem.* **21** (2000) 132–146.

[20] S. Jana and J. Deb, Molecular understanding of aminoglycoside action and resistance. *Appl. Microbiol. Biotechnol.* **70** (2006) 140–150.

[21] M. Kaul and D.S. Pilch, Thermodynamics of Aminoglycoside-rRNA Recognition: The Binding of Neomycin-Class Aminoglycosides to the A Site of 16S rRNA. *Biochemistry* **41** (2002) 7695–7706.

[22] M. Kaul, C.M. Barbieri, J.E. Kerrigan and D.S. Pilch, Coupling of Drug Protonation to the Specific Binding of Aminoglycosides to the A Site of 16S rRNA: Elucidation of the Number of Drug Amino Groups Involved and their Identities. *J. Mol. Biol.* **326** (2003) 1373–1387.

[23] M. Kaul, C.M. Barbieri and D.S. Pilch, Defining the Basis for the Specificity of Aminoglycoside-rRNA Recognition: A Comparative Study of Drug Binding to the A Sites of Escherichia coli and Human rRNA. *J. Mol. Biol.* **346** (2005) 119–134.

[24] S. Kevin, Energy landscape of the ribosomal decoding center. *Biochimie* **88** (2006) 1053–1059.

[25] J. Kondo, B. François, R.J. Russell, J.B. Murray and E. Westhof, Crystal structure of the bacterial ribosomal decoding site complexed with amikacin containing the gamma-amino-alpha-hydroxybutyryl (haba) group. *Biochimie* **88** (2006) 1027–1031.

[26] J. Kondo, M. Koganei and T. Kasahara, Crystal Structure and Specific Binding Mode of Sisomicin to the Bacterial Ribosomal Decoding Site. *ACS Med. Chem. Lett.* **3** (2012) 741–744.

[27] M. Kulik, A.M. Goral, M. Jasiński, P.M. Dominiak and J. Trylska, Electrostatic interactions in aminoglycoside-RNA complexes. *Biophys. J.* **108** (2015) 655–665.

[28] C. Ma, N.A. Baker, S. Joseph and J.A. McCammon, Binding of Aminoglycoside Antibiotics to the Small Ribosomal Subunit: A Continuum Electrostatics Investigation. *J. Am. Chem. Soc.* **124** (2002) 1438–1442.

[29] S. Meroueh and S. Mobashery, Conformational transition in the aminoacyl t-RNA site of the bacterial ribosome both in the presence and absence of an aminoglycoside antibiotic. *Chem. Biol. Drug. Des.* **69** (2007) 291–297.

[30] J. Panecka, M. Havrila, K. Réblová, J. Šponer and Joanna Trylska. Role of S-turn2 in the Structure, Dynamics, and Function of Mitochondrial Ribosomal A-Site. A Bioinformatics and Molecular Dynamics Simulation Study. *J. Phys. Chem. B* **118** (2014) 6687–6701.

[31] P. Pfister, S. Hobbie, C. Brüll, N. Corti, A. Vasella, E. Westhof and E.C. Böttger, Mutagenesis of 16S rRNA C1409-G1491 base-pair differentiates between 6'OH and 6'NH3+ aminoglycosides. *J. Mol. Biol.* **346** (2005) 467–475.

[32] D.S. Pilch, M. Kaul, C.M. Barbieri and J.E. Kerrigan, Thermodynamics of aminoglycoside-rRNA recognition. *Biopolymers* **70** (2003) 58–79.

[33] J. Romanowska, P. Setny and J. Trylska, Molecular Dynamics Study of the Ribosomal A-Site. *J. Phys. Chem. B* **112** (2008) 15227–15243.

[34] D.H. Ryu and R.R. Rando, Aminoglycoside binding to human and bacterial A-Site rRNA decoding region constructs. *Bioorg. Med. Chem.* **9** (2001) 2601–2608.

[35] A.C. Vaiana, E. Westhof and P. Auffinger, A molecular dynamics simulation study of an aminoglycoside/A-site RNA complex: conformational and hydration patterns. *Biochimie* **88** (2006) 1061–1073.

[36] A. Vaiana and K. Sanbonmatsu, Stochastic gating and drug-ribosome interactions. *J. Mol. Biol.* **386** (2009) 648–661.

[37] Q. Vicens and E. Westhof, Crystal structure of paromomycin docked into the eubacterial ribosomal decoding A site. *Structure* **9** (2001) 647–658.

[38] Q. Vicens and E. Westhof, Crystal Structure of a Complex between the Aminoglycoside Tobramycin and an Oligonucleotide Containing the Ribosomal Decoding A Site. *Chem. Biol.* **9** (2002) 747–755.

[39] Q. Vicens and E. Westhof, Crystal structure of geneticin bound to a bacterial 16S ribosomal RNA A site oligonucleotide. *J. Mol. Biol.* **326** (2003) 1175–1188.

[40] Q. Vicens and E. Westhof, Molecular recognition of aminoglycoside antibiotics by ribosomal RNA and resistance enzymes: an analysis of x-ray crystal structures. *Biopolymers* **70** (2003) 42–57.

[41] H. Wang and Y. Tor, Electrostatic Interactions in RNA Aminoglycosides Binding. *J. Am. Chem. Soc.* **119** (1997) 8734–8735.

[42] J. Wang, P. Cieplak and P.A. Kollman, How well does a restrained electrostatic potential (RESP) model perform in calculating conformational energies of organic and biological molecules? *J. Comput. Chem.* **21** (2000) 1049–1074.

[43] C.-H. Wong, M. Hendrix, E.S. Priestley and W.A. Greenberg, Specificity of aminoglycoside antibiotics for the A-site of the decoding region of ribosomal RNA. *Chem. Biol.* **5** (1998) 397–406.

[44] G. Yang, J. Trylska, Y. Tor and J.A. McCammon, Binding of aminoglycosidic antibiotics to the oligonucleotide A-site model and 30S ribosomal subunit: Poisson–Boltzmann model, thermal denaturation, and fluorescence studies. *J. Med. Chem.* **49** (2006) 5478–5490.